Theoretical evaluation of the spark-ignition premixed oxy-fuel combustion concept for future CO_2 captive powerplants

J.R. Serrano[a], J. Martín[a,*], J. Gomez-Soriano[a], R. Raggi[a]

[a] *CMT – Motores Térmicos, Universitat Politècnica de València, Camino de Vera, 46022 Valencia, Spain*

Abstract

Oxy-fuel combustion concept is one of the most promising technologies not only to avoid NO_x emissions, but also to reduce CO, unburned hydrocarbons and soot emissions in combustion-based powerplants. Moreover, the concept facilitates Carbon Capture and Storage (CCS), thus promoting CO_2 integration in a circular economy strategy (i.e. e-fuels production). For O_2 production, mixed ionic-electronic conducting membranes (MIEC) arise as a solution to separate pure O_2 from air, but its thermal requirements must be considered in order to guarantee its integration with the internal combustion engine (ICE). In this study, the combustion process using pure oxygen as oxidizer is studied in a spark ignition ICE. A numerical method to assess the combustion process and engine outputs in oxy-fuel operation, taking into account the thermo-mechanical constraints, is developed and validated with experiments. It has been concluded that the use of EGR is more appropriated than O_2 for diluting the oxidizer, and the best operating strategy consist in using stoichiometric conditions and 60% to 70% EGR rate, thus having a good compromise between combustion stability and efficiency, engine integrity, and MIEC operation. It is also shown that oxy-fuel combustion reduces knocking propensity and hence, on the one hand, it provides some room for spark optimization, specially at high load; on the other hand, it allows increasing compression ratio. Both strategies are interesting to compensate the expected fuel consumption increase observed in oxy-fuel operation.

Keywords: *Oxy-fuel combustion, CO_2 capture, MIEC, CCS, ICE*

1. Introduction

In the last years, the world's major economies have actively pursued sustainable development plans in which the different productive sectors maintain their activities on a regular basis in a way that is more efficient and less harmful to the environment. An example of this is the EU climate and energy framework with 2030 targets and policies [1], whose main objectives are to reduce greenhouse gas emissions by 40% (CO_2, HC_4, N_2O, fluorinated gases, etc.) and to increase by 32.5% the energy efficiency within the European territory. Likewise, global societies are working to improve life quality in large cities by reducing emissions of gases and other substances which are harmful for human health (H_xC_y, NO_x and particulate matter).

Among the sectors with the highest gases emission, road transport and maritime international shipments can be highlighted [2, 3], representing 25% and 13% of greenhouse gas emissions in Europe, respectively. For this reason, the policies implemented by the European Union in these sectors prioritize increasing the efficiency of the systems that integrate these areas, the development of new fuels with low environmental impact (e-fuels, and bio-fuels) and the develop of propulsive systems with low or no emissions.

Related to the generation of these emissions, carbon oxides (CO, CO_2) are generated due to the use of hydrocarbons in the combustion process, which are the main components of the fuels used in internal combustion engines (ICE), while nitrogen oxides (NO_x) are generated due to the presence of nitrogen in the air used as oxidizer in combination with the high temperatures reached that promote its oxidation.

One of the possible solutions to mitigate these problems could be the electrification of vehicles, which would achieve low local emissions on propulsion systems, but it should be noted that electric engines present difficulties in solving the problems of autonomy and recharging time when they are used on extra-urban routes, and thermal dissipation of critical components that leads to performance reduction [4]. Those problems decrease when they are hybridized with an ICE which can also act as a range extender or simply as a generator of electrical energy to charge the batteries [5, 6]. Several works [7, 8, 9] studied methodologies based on models that allow a better and faster design of the different systems (electrical system, combustion engine or other auxiliary systems) that make up the hybrid drive. Despite the improvement from the point of view of energy efficiency and global pollutant emissions compared to powertrains with only a combustion engine, these hybrid systems still have a traditional ICE engine that produce polluting gaseous emissions [10].

*Corresponding author.
email: jaimardi@mot.upv.es

Considering the technologies that are under development nowadays, industrial experience has shown that oxy-fuel combustion could be one of the most promising due to the significant reduction not only of NO_x emissions [11, 12], but also of CO, H_xC_y and particulate matter (soot and unburned hydrocarbons) coming from the incomplete combustion in the ICE. Oxy-fuel combustion is defined as the combustion process produced in a highly O_2-enriched ambient, in which high temperature can be controlled by means of a dilution gas such as Exhaust Gas Recirculation (EGR), mainly composed of CO_2 and H_2O vapor, instead of N_2. Among the most promising benefits of oxy-fuel combustion, there is the possibility of capturing CO_2 [13] to be used as a by-product in circular economy strategies, for example in the synthetic fuels and e-fuels production. Moreover, previous research have shown improvement in power generation and reduction of polluting emissions with oxy-fuel combustion applied to ICE [14, 15], to electricity generation plants [16, 17, 18] and to industrial processes [19, 20].

Nevertheless, this combustion concept has also drawbacks, being the oxygen supply the main of them. In stationary applications, its acquisition may not be a suitable solution for the industry due to provisioning, storage and transport costs. Also, it is an issue for transport applications since it would require an increment of weight in vehicles leading to a fuel consumption deterioration. Even though more complex and expensive systems on board are required, high-purity oxygen separation is a promising technical solution to be explored for oxy-fuel combustion in transport applications. Between the different options mixed ionic-electronic conducting membranes (MIEC) found to be well suited for transport application options, where in particular $Ba_{0.5}Sr_{0.5}Co_{0.8}Fe_{0.2}O_3$-$\delta$ (BSFC) membranes has a high oxygen permeation with production capacity of up to 62 ml/min/cm^2 of oxygen [21]. Serra et al. [22] conducted a characterization study of oxygen transport on MIEC BSFC based on experimental and numerical assessment, analysing some effects such as MIEC temperature feeding flow, sweep inlet flow and sweep gas composition. Their results show that increasing the temperature from 700°C to 1000°C improve the oxygen transport through the membrane and thus its production rate. This temperature range to produce the O_2 was assumed as a key boundary condition in order to couple the membrane to the ICE. In this line, Desantes et al. proposed a patent combining a MIEC in a syniergical way with an ICE in order to use the waste heat from the engine to provide the required thermal power for the membrane [23].

In this context, this paper has two main objectives. On the one hand, assessing the dilution conditions (in terms of λ and EGR) where oxy-fuel combustion can be used in a spark ignition engine (SI), taking into account thermo-mechanical limitations in the chamber and knocking. To this end, a numerical method is proposed and validated with experiments to assess oxy-fuel combustion features. The second main objective is to assess the potential of this particular combustion concept in optimal conditions, from the indicated efficiency point of view, identifying its main benefits and drawbacks. Finally, the viability of the system integration (ICE + membrane) is briefly discussed.

This paper is structured as follows: the next section presents the experimental setup and the simulation tools used along with its respective validation. Section three describes the numerical method implemented to study the oxy-fuel combustion applied to ICEs. In section four results are presented and analyzed to define the thermo-mechanical limitation, and the best dilution strategy for this combustion concept is defined. Also, an assessment of the performance and a comparison with conventional combustion is discussed. Finally, the last section summarizes the conclusions of the paper and remarks its main contributions.

Table 1: *Main engine specifications.*

Number of cylinders	1
Injection system	PFI (up to 8 bar)
Ignition system	Spark (spark plug)
Number of strokes	4
Cylinder displacement	454.2 mm
Compression ratio	10.7
Cylinder diameter	82.0 mm
Stroke	86.0 mm
Connecting rod length	144.0 mm

2. Experimental and simulation tools

Experimental tests for the models validation were performed in a SI single-cylinder engine specifically developed for research purposes. The engine was equipped with a port injection system (PFI) that was used to avoid additional uncertainties related to the charge inhomogeneities. Table 1 contains the main characteristics of the engine.

The engine was assembled in a test cell instrumented according to the scheme presented in Fig. 1. The original layout of the test bench was adapted for supplying O_2 and CO_2 from two different tanks. The latter was specifically installed for providing the required oxidant dilution to keep engine integrity during the engine start-up; once a steady operation was reached, the external supply of CO_2 was substituted by EGR. Moreover, the system was designed in order to be flexible to switch between conventional combustion and oxy-fuel combustion operation mode, being the valve located downstream the intake settling chamber, and the CO_2 and O_2 flows control vales the ones used for this purpose. For conventional combustion cases, an external compressor is used in order to provide the compressed air to reproduce boost conditions.

The exhaust back-pressure was controlled by a knife-gate valve located after the exhaust settling chamber in the exhaust line. Demanded levels of cooled EGR were provided by a high pressure EGR system. Oil and cooling circuits were independent from the engine as depicted in the layout.

In-cylinder pressure was measured using a piezoelectric sensor. An additional piezoresistive pressure sensor was installed at the cylinder liner close to the bottom dead center

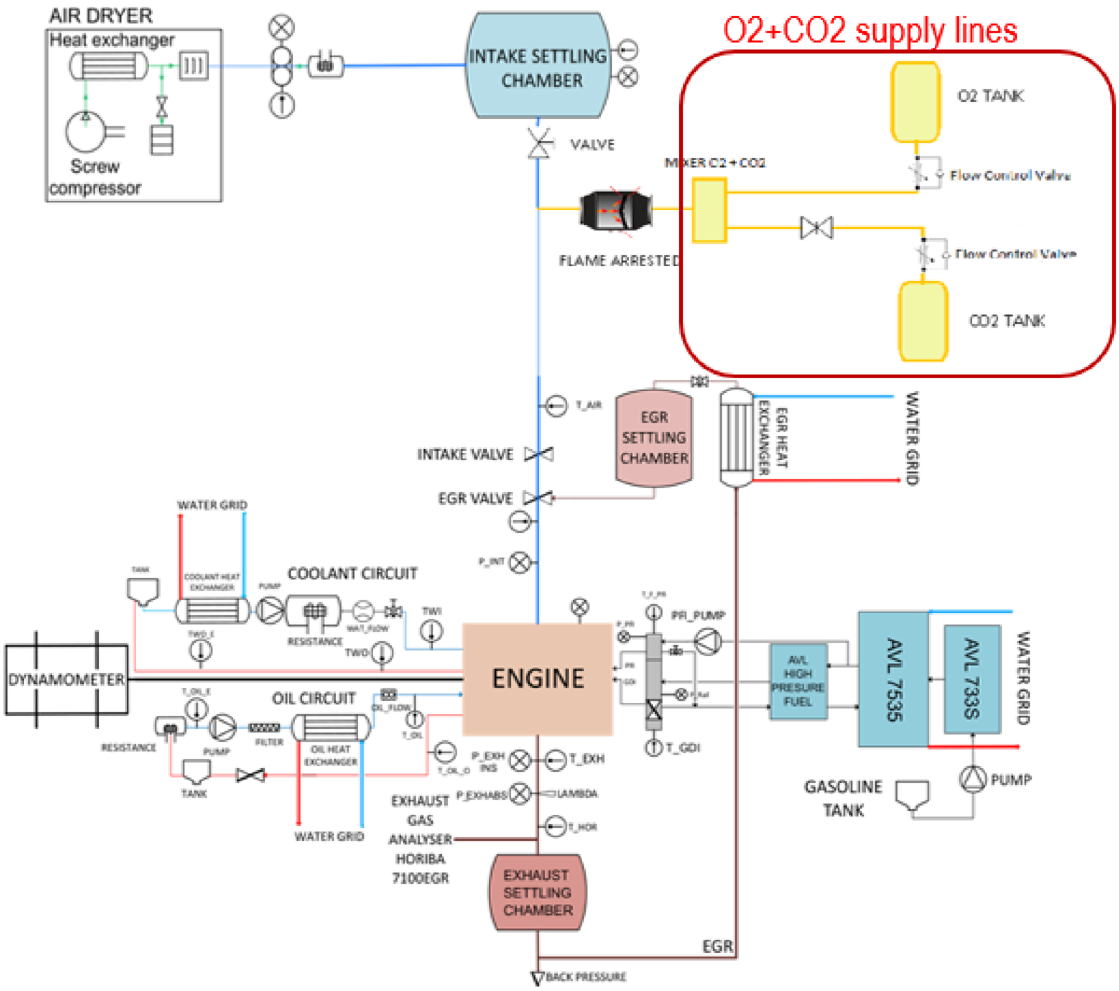

Figure 1: *Layout of the engine test cell.*

for the pressure signal pegging. Moreover, to adquire the intake and exhaust intantaneous pressure, two piezoresistive sensors were mounted. All engine fluid temperatures were controlled and monitored during the experimental tests using K-type thermocouples. NO_x emissions and CO_2 concentration (to calculate the EGR rate) were measured by a HORIBA MEXA-7100EGR gas analyzer. Complete details about the instrumentation and its accuracy are summarized in Table 2.

The global parameters related to the combustion process, i.e. the indicated mean effective pressure (IMEP), combustion phasing, maximum cylinder pressure, combustion misfiring, cycle-to-cycle variability (CoV_{IMEP}) and Heat Release Rate (HRR) were obtained from the in-cylinder pressure signal by the thermodynamic combustion diagnosis tool CALMEC [24, 25].

2.1. Computational tools

2.1.1. Chemistry modelling

Auto-ignition delay and flame temperature for different fuel-oxidizer mixtures and thermodynamic conditions were estimated by using zero-dimensional (0D) chemistry calculations. Data generated using a well-stirred reactor model, assuming constant pressure, were used for predicting the knocking combustion tendency and maximum local temperatures. The ignition delay timing was defined as the time required for increasing 400K from its initial temperature [26].

The chemical kinetic mechanism proposed by Liu et al. [27], based on a Primary Reference Fuel (PRF), was chosen for its good balance between accuracy and computational requirements. Benajes et al. [28] demonstrated the capabilities of this mechanism under realistic and representative engine conditions, validating its results against the experimental data reported by Fieweger et al. [29].

The laminar flame speed of an oxidation reaction can be estimated by considering a freely propagating flame in a channel with fixed cross-sectional area for a specified temperature, pressure and mixture composition. Although this parameter is traditionally calculated by using empirical correlations [30, 31], they systematically tend to under-predict the laminar flame speeds at realistic engine conditions [28]. Thus, a 1D laminar flame speed solver was used to get more accurate predictions. Again, the chemical kinetic mechanism

Table 2: *Summary and accuracy of the instrumentation used in the experiments.*

Variable	Sensor	Accuracy
In-cylinder pressure	Piezoelectric sensor	0.2%
Temperature of all fluids	Thermocouples (K-type)	1.5ºC
Engine speed	Encoder	3 rpm
CO_2 and NO_x concentration	Exhaust gas analyzer	3.0%
Intake, exhaust & pegging	Piezoresistive	0.35%
Torque	Torque meter	0.1 Nm
Fuel mass flow	Fuel mass flow meter (AVL 733S)	0.2%
Air mass flow	Air mass flow meter (Sensiflow D80)	2.0%

from Liu et al. [27] was selected, due to its consistence with the experiments performed by Jerzembeck et al. [32] and Heimel et al. [33].

2.1.2. 0D-1D Thermodynamic model: description and validation

0D-1D tools show a good compromise between accuracy and computation time [34, 35]. To characterise the premixed oxy-fuel combustion concept, the in-cylinder pressure and temperature, gross indicated efficiency (GIE) and exhaust temperature under different EGR dilutions were simulated with a 0D-1D tool. The engine and test bench layout were implemented in the GT-SUITE code. These simulations allowed reducing experimental test campaigns while evaluating different strategies to implement in the engine. In addition, a PID-controller was implemented to optimize the GIE by changing the start of combustion (SoC) while keeping the maximum in-cylinder pressure below 150 bar.

The model was initially calibrated using experimental data from the same engine operating under conventional SI conditions at 3000 rpm and for two different loads (4 and 11 bar of IMEP). In both cases, the combustion process was reproduced by imposing the heat release rate obtained by the combustion diagnosis tool [24, 25] previously described. Results of the validation are summarized in Figs. 2 and 3. Here, the measured in-cylinder pressure and temperature (estimated by the combustion diagnosis tool) are compared against simulations, showing a reasonable agreement in both operating conditions considered so far.

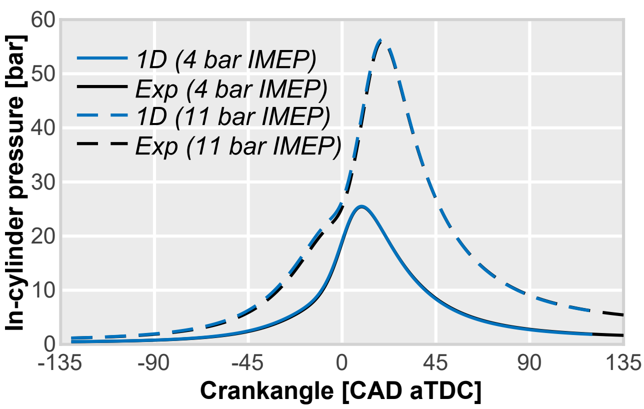

Figure 2: *Experimental and simulated in-cylinder pressure at two operating conditions.*

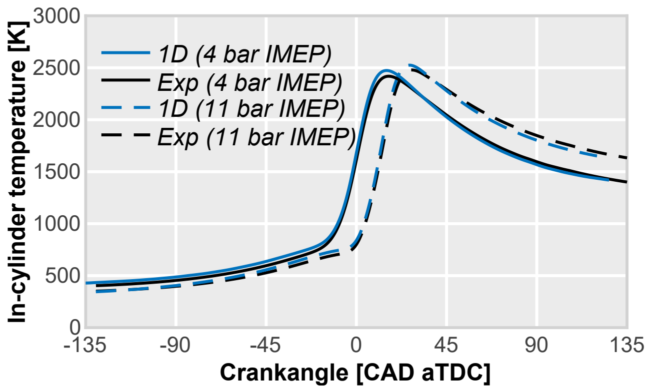

Figure 3: *In-cylinder temperature comparison at two operating conditions.*

2.1.3. CFD model: description and validation

CFD simulations were carried out using the CONVERGE v2.4 CFD software [36], a commercial code based on the finite volume method and particularly developed for ICE applications. The model was built from the real engine geometry, considering the combustion chamber and both intake/exhaust ports.

As shown in Fig. 4, an hexahedral grid strategy based on a orthogonal basis was used for meshing the complete computational domain with a base cell size of 4 mm. The mesh was refined up to 2 mm in the intake and exhaust, and up to 1 mm in the cylinder. The cell resolution was increased (0.5 mm) near the cylinder walls, including the moving piston and valves. Additionally, an Adaptive Mesh Refinement (AMR) algorithm was used to increase the grid resolution where spatial gradients of velocity and temperature are meaningful. This algorithm considered a sub-grid criteria of 1 m/s and 2.5 K to decrease the cell size up to a minimum of 0.125 mm. Finally, the grid resolution was further increased by reducing mesh size down to 0.0625 mm at the spark gap electrodes to capture the initial flame kernel development. Full details about the grid definition are given in Table 3.

Turbulence modelling was performed under the unsteady Reynolds-averaged Navier–Stokes (URANS) framework. In particular, the Re-Normalization Group variant of the k-epsilon model (RNG k-ϵ model [37, 38]), based on an eddy-viscosity-based two-equation turbulence model, was used. The gas-to-

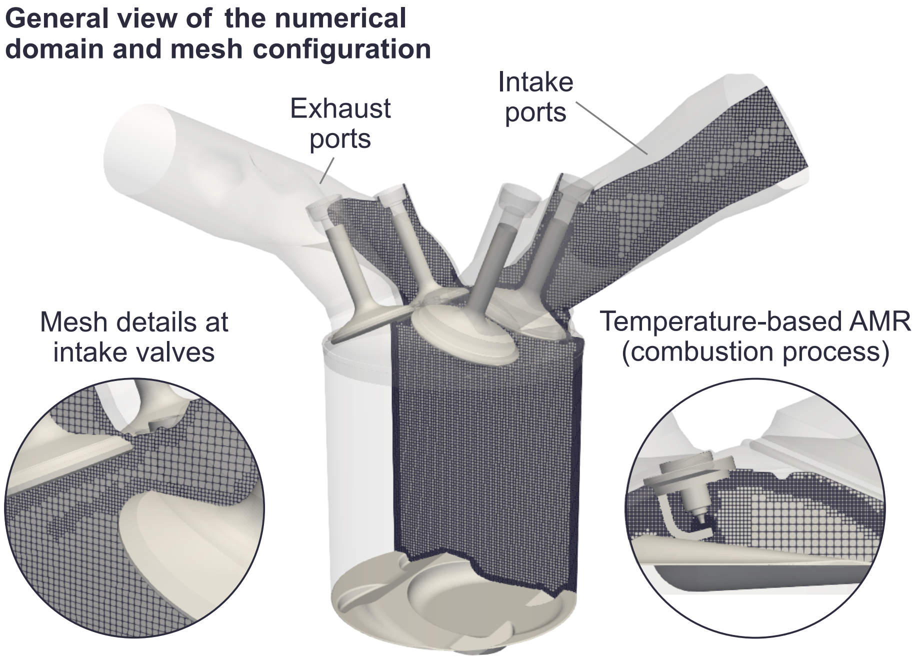

Figure 4: *Numerical domain and mesh characterization of the engine architecture.*

Table 3: *Mesh configuration details.*

Base size	4 mm
Intake/exhaust ports	2 mm
Chamber refinement	1 mm
Walls refinement	0.5 mm
AMR min. size	0.125 mm
Spark refinement	0.0625 mm
Number of cells	0.5-4 million

wall heat transfer was modelled by the approach proposed by Angelberger [39]. This combination has been widely used in ICE applications [40, 41].

The simulations were performed using a second-order central difference scheme for spatial discretization and a first-order scheme for temporal discretization. A Pressure Implicit with Splitting of Operators (PISO) algorithm modified by [42] was considered for the pressure and velocity fields coupling. The ideal gas equation of state was selected for calculating the compressible flow properties.

The detailed chemistry solver [43] was combined with a multi-zone (MZ) approach for combustion modelling, considering 5K temperature bins [44]. Previous studies [45] demonstrated the suitability of this approach for URANS-based gasoline combustion, even considering that it does not use an explicit turbulent combustion closure [46]. As in the 0D-1D chemistry simulations, the chemical kinetic mechanism proposed by Liu et al. [27] was used for mimicking the thermo-chemical properties of the fuel. The spark kernel was modelled by a volumetric source located between the spark plug electrodes. An energy deposition of 40 mJ was spatially and uniformly distributed in a sphere of 0.5 mm along a L-type profile [47].

The inflow and outflow boundary conditions located at the end of the intake/exhaust ports were defined by the instantaneous pressure signal measured in the engine tests. The surface temperatures of all wall boundaries were predicted by a lumped model [48].

The model was validated by the same experimental data used in the validation of the 0D-1D thermodynamic model. A comparison between experiments and CFD-simulated results at 3000@11 is shown in Fig. 5. Again, a reasonable prediction of the in-cylinder pressure and HRR signals was achieved.

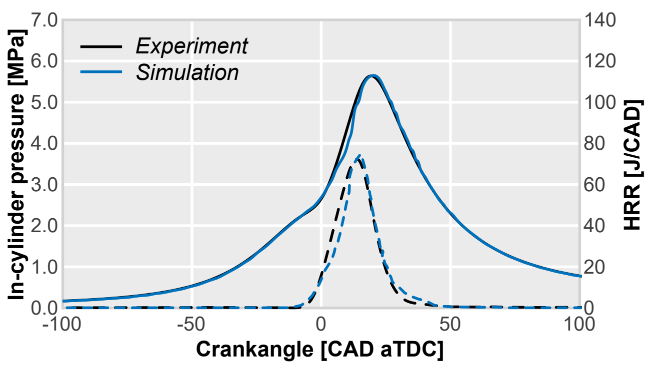

Figure 5: *Validation of CFD simulations at 3000 rpm and 11 bar IMEP. In-cylinder pressure signal and HRR trace are considered in the process.*

3. Methodology

The numerical method is divided into four different steps. First, a representative sample for the engine operation is selected. Then, details about the estimation of the engine thermo-mechanical limits are given. Afterwards, the coupling between the 0D-1D model (GT-SUITE) and the CFD code for the engine outcomes assessment is explained. Finally, the effectiveness of the method is verified by real oxy-fuel combustion engine experiments.

3.1. Operating conditions

A set of operating conditions shown in Table 4 was chosen to find a good compromise between the number of simulations and the expected outcomes. These operating conditions are characterized by a constant engine speed of 3000 rpm and different levels of engine load (3.7, 10.7 and 21.4 bar of IMEP). In addition to the operating parameters, the most relevant experimental conditions are also detailed in Table 4. It is worth to mention that low and medium engine load (3.7 and 10.7 bar of IMEP respectively) were measured in the test bench, while the high load operating point was only simulated.

Table 4: *Operating parameters of the reference operating conditions using conventional SI combustion at stoichiometric conditions.*

Operating point	Point 1	Point 2	Point 3*
Engine speed [rpm]	3000	3000	3000
IMEP [bar]	3.7	10.7	21.4
Injected fuel quantity [mg/cc]	10.6	33.15	66.3
Spark timing [CAD]	-16.6	-19	-19
Coolant temperature [°C]	80	85	85
Oil temperature [°C]	90	92	92
Intake pressure [bar]	0.41	0.98	1.37
Intake temperature [°C]	31	33	38

*Simulated.

3.2. Definition of thermo-mechanical limits

A preliminary evaluation of the concept was performed by a combination of thermodynamic relationships and 0D-1D chemistry calculations (from now on referred as chemistry calculations to differentiate it from the one obtained with the GT-SUITE tool). Particularly, the maximum flame temperature, the laminar flame speed and the chemical auto-ignition delay (AID) were analysed and compared between conventional combustion and oxy-fuel combustion. The aim of this study was to identify the most interesting dilution strategy (O_2 or EGR) for oxy-fuel combustion and to determine the effective operating range that fulfills the mechanical and thermodynamic constraints.

This study was based on the reference values obtained from the conventional combustion as:

- The maximum flame temperature using oxy-fuel combustion was established at 3000 K, which corresponds to the flame temperature obtained at stoichiometric and non-diluted conditions. Boundary conditions for the chemical calculations were estimated by the engine signals (pressure and mixture composition), the GT-SUITE model and the combustion diagnosis tool (bulk temperature). Due to the lack of experimental data for Point 3 (Table 4), boundary conditions were estimated from data of Point 2.

- The combustion stability threshold was obtained from the laminar flame speed estimated at the dilution limits experimentally obtained operating with conventional combustion in the bench, when a high dilution strategy is considered (using both air and EGR dilution). As in the previous criterion, boundary conditions are set by the engine measurements at stoichiometric conditions. Since the combustion duration at these extreme conditions fluctuates between 40 and 50 CAD, the threshold was established at 45 CAD (2.5 ms). Considering that the spark plug is located at the center of the cylinder, it is possible to relate the laminar flame speed with the distance to travel by the flame front and the time to reach the cylinder wall if the contribution of the turbulence is constant. Therefore, an estimation of the minimum laminar flame speed that ensures a reasonable combustion duration and stability can be obtained.

- The knock propensity is qualitatively assessed by considering the AID of the reference stoichiometric case. An AID below this reference value means that the knock tendency is higher than in the conventional gasoline combustion and *vice versa*.

3.3. Assessment of the engine outputs

Once the most interesting operating settings and conditions were identified, the performance of the concept was assessed by a virtual version of the engine implemented in GT-SUITE. This model accounts for both the gas exchange and in-cylinder processes with a complete recreation of the test bench facility including the engine and all auxiliary components.

One of the main drawbacks of these simplified models is the uncertainty of combustion modelling. The complexity of this process and its strong 3D nature compromises the accuracy of current 0D and 1D models. If dilution strategies or the oxidizer change are included in the equation, this uncertainty can be even higher.

In order to improve this situation, the virtual engine was coupled with the 3D CFD model through an iterative procedure, where the flow of information between them is bidirectional:

- Results provided by the 1D simulation of the research single cylinder engine allow setting the boundary conditions for the CFD modelling.

- The heat release law obtained with CFD modelling under different operating conditions is fed back to the 1D model to assesst the performance of the oxy-fuel combustion concept.

Using this approach, described in detail below, the impact of both dilution rate and spark timing was evaluated at the operating conditions presented in Table 4.

The iterative procedure is illustrated in Fig. 6 for the 3000-@11 operating point. To initialize the first iteration, an experimental conventional combustion heat release was assumed to calculate the thermodynamic gas evolution with GT-SUITE that was used to impose the boundary conditions in CFD calculations. Once the 3D reacting simulation was finished, considering the closed-cycle only, the 1D virtual engine was fed with this new combustion profile. After 2 or 3 iterations, depending on the operating condition, the differences of the combustion characteristic parameters such as the peak of the heat release and the combustion duration were no longer significant, meaning that the convergence between both codes was reached.

Finally as an additional study to show the potential of the proposed iterative method, the indicated performance of the closed cycle was optimized by acting on the ignition advance through a PID controller implemented in the 1D model, in order to modify the combustion centering. Moreover, in this optimization a limit value of the maximum cylinder pressure of 150 bar was established as a restriction, consistent with the engine specifications.

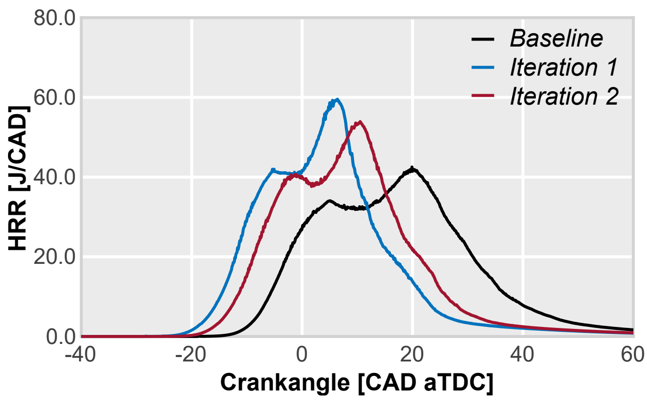

Figure 6: *Evolution of the combustion law though the iterative process obtained from CFD simulations at 3000 rpm, 11 bar of IMEP and 70% of EGR.*

3.4. Validation of the methodology

As a final step, the reliability of the numerical method is verified by comparison with oxy-fuel combustion experiments performed in the test bench. In Fig. 7, the variables simulated with the described 0D-1D-CFD method are compared to the measured ones at 3000@11 operating point applying a 70% EGR dilution with 850 mbar and 303 K of intake pressure a temperature respectively. Although there are certain differences in the peak of HRR, results reasonably mimic the pressure evolution and accurately predict both the start and the duration of the combustion process. Considering that none of the sub-models have been specifically adjusted for oxy-fuel combustion operation, results are promising and the method can be used for preforming further studies.

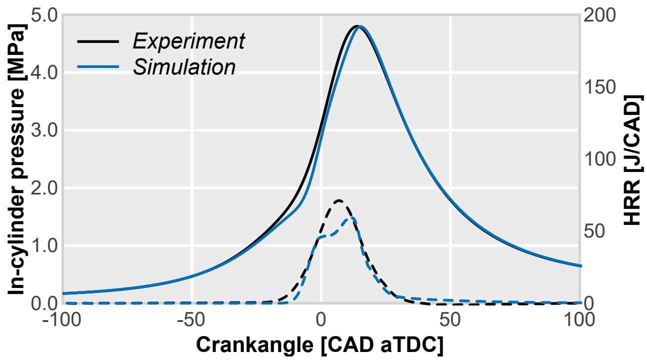

Figure 7: *Validation of the numerical method for oxy-fuel combustion. The in-cylinder pressure signal and HRR trace obtained form CFD simulations at 3000 rpm, 11 bar of IMEP and 70% of EGR are contrasted.*

Thus, the numerical procedure has demonstrated to be a fast and effective way to obtain the engine outputs when operating with oxy-fuel combustion at maximum GIE conditions with different levels of EGR, allowing the analysis of the engine performance and thus, assessing the feasibility of the concept.

4. Results and discussion

Results are presented in three different subsections, each one of them fulfilling the specific objectives described in the introduction. The thermo-mechanical limits of the engine during a suitable oxy-fuel combustion operation are established first by the chemical simulations. Then, the stability and safety thresholds are verified by the 0D-1D/CFD coupling method. In particular, the sensitivity to EGR dilution is studied and the appearance of abnormal combustion (knocking) at high engine load is evaluated. Finally, the global engine parameters of oxy-fuel combustion are assessed and contrasted to those obtained by the conventional SI combustion concept.

4.1. Assessment of dilution rates

To provide an overview on which operating settings are meaningful and interesting from the point of view of the oxy-fuel combustion operation, multiple sets of chemical simulations were performed. The aim was to identify the most favorable strategy for dilution (O_2 and/or EGR) and to give an idea about the effective ranges of variation. In Fig. 8, both the O_2 (lambda) and EGR dilution rates were swept.

As a first step, a preliminary evaluation of the oxy-fuel combustion concept was carried out using a combination of thermodynamic analysis and chemical calculations [49], with the aim of identifying the strategy with the most appropriate dilution and safe operating range to avoid exceeding the thermal and mechanical limitations of the engine. This way, it is ensured that the subsequent experimental start-up of the engine is safe and the starting point for the experimental matrix is focused on the interesting condition obtained from the simulated database.

Fig. 8 shows the effect of changing the two fundamental parameters (independent input variables) that allow controlling the composition of the oxidizer (and therefore the dilution of the charge in the cylinder): the rate of recirculated gases (EGR) and the O_2-fuel ratio or lambda (λ). The output variables analyzed are the adiabatic flame temperature, the laminar flame speed and the AID time, which are the most relevant parameters for the characterization of the combustion process in the engine. For each dilution condition, characterized with EGR and λ, chemical calculations were performed to estimate the three mentioned parameters.

Figure 8 shows the results for the medium speed/load operating point (3000 rpm and 11 bar IMEP, 3000@11). As it can be seen, working with a pure O_2 dilution strategy (without considering EGR) the engine must be operated between λ values of 5 and 7 to avoid, simultaneously, exceeding thermal limitations and preventing performance degradation due to excessively low burning rates. Such analysis was also performed for a low load condition, to check if trends are similar. In Fig. 9, results are shown for less demanding conditions: 3000 rpm and 4 bar IMEP, 3000@4. Results show the same trends observed for the point 3000@11. Focusing on the bottom graph of Figs. 8 and 9, the knock tendency can be observed. Results of AID show a slight tendency towards higher knock propensity when there is a decrease of the EGR and an increase of λ dilution. Despite not being so critical, this may be the first reason to think about applying dilution strategies with EGR. A second reason, is that the production of O_2 is costly from the point of view of energy consumption. And a third reason is that with λ values much higher than 1, the $O_2 + CO_2$ mixture will need temperatures much lower than 303 K for CO_2 liquefaction, in order to storage it before capture.

For the case of diluting only with EGR while considering stoichiometric λ, the suitable range for dilution vary from 65% to 75%. Keeping the EGR rate above 65%, the adiabatic flame temperatures do not exceed the engine material limits (3000K). Moreover, it is not possible to operate with dilutions larger than 75% because the burning rate slows down to levels where the flame can be extinguished. Following this dilution strategy, should not be knocking-related problems considering both operating conditions.

If a combined dilution strategy with $\lambda > 1$ and EGR is used, there is a combined effect of the trends commented before. As λ is reduced from 5 to 1 the EGR rate must be increased from 0% to 65% minimum for both operating points (low and medium load) to keep the adiabatic temperature limit below 3000 K. Similarly, λ must be reduced from 7 to 1 as the EGR must be increased from 0 to 75% to maintain a suitable combustion stability.

With the analysis of these chemical simulations, it has been identified the potential λ and EGR ranges where the oxy-fuel combustion concept can be applied with the imposed restrictions. In order to achieve high λ values, the production of O_2 in the MIEC must be increased significantly, thus requiring higher energy demand for the membrane operation. Moreover, this strategy will difficult the capture of CO_2 from the exhaust gases, since its separation from $O_2 + H_2O$ is not trivial.

From a technological point of view, EGR is a conventional strategy, already implemented in standard engines, and several ways of achieving the required EGR rates has been describes in the patent of Desantes et al. [23] about a multicylinder oxy-fuel combustion engine. Therefore, it is energetically more efficient to control combustion temperature by getting required EGR rates than required lambda values. Due to these reasons and that high concentrations of CO_2 in the exhaust gases facilitates the thermal and energetic feasibility of in-situ O_2 production with MIECs and of CCS technologies [50], the oxy-fuel combustion concept was evaluated by using EGR dilution (60%-75%) at stoichiometric conditions ($\lambda \approx 1$).

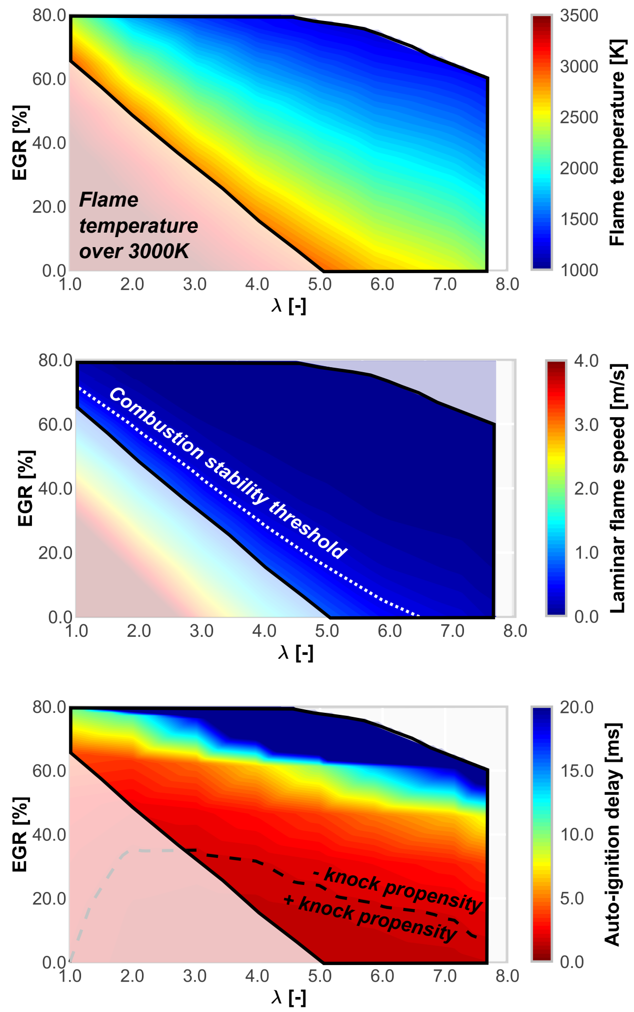

Figure 8: *Analysis of chemical simulations at 3000 rpm and 11 bar IMEP.*

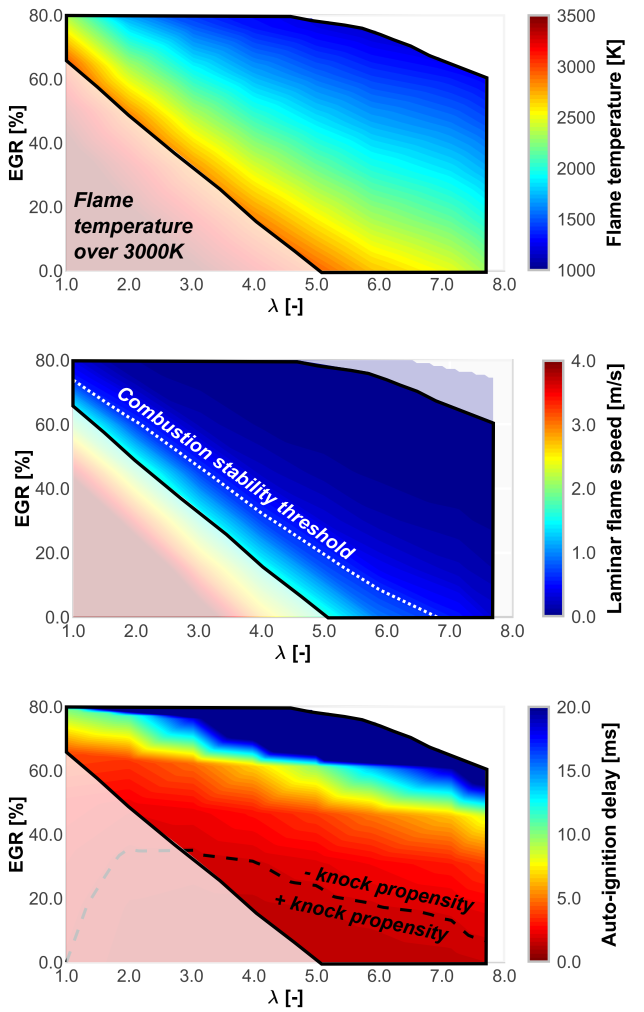

Figure 9: Analysis of chemical simulations at 3000 rpm and 4 bar IMEP.

4.2. Verification of stability and safety thresholds

4.2.1. Impact of EGR dilution on combustion

After analyzing the results obtained with the chemical simulations in the previous section, it was possible to focus the study of the oxy-fuel combustion concept on a specific area of interest in the λ- EGR map. Specifically, diluting with EGR while keeping stoichiometric conditions seems to be the most favourable strategy to minimize the energy required by the MIEC for the oxygen production.

Since understanding combustion phenomena is essential to ensure the stability and maximize the benefits of oxy-fuel combustion, more accurate simulations are required to reproduce in detail the physical phenomena related to combustion. Due to the simplifications considered in the chemical models, the 3D CFD model was used to predict a realistic combustion law operating under oxy-fuel combustion conditions.

In Figs. 10 and 11, the instantaneous evolution of the in-cylinder pressure and the rate of heat release (HRR) calculated for different dilution levels are drawn. Three levels of EGR were simulated (60%, 65% and 70%) keeping the same ST in Fig. 10 and the same combustion centring (characterized through angle at which 50% of the fuel mass is burned -CA50-) in Fig. 11. In addition to the simulated oxy-fuel results obtained for the 3000@11 operating point, the experimental evolution of equivalent conditions using conventional SI combustion (same fuel mass, $\lambda = 1$, no EGR) are also included in these figures. It is observed that, for a constant spark timing, the combustion accelerates as the dilution rate decreases, exhibiting a shorter combustion duration and higher heat release peak (up to 60 J/CAD of difference). The duration of the conventional combustion is close to the 60% case. As expected from the analysis of the previous section, combustion tends to degrade as the dilution increases, reaching a critical value around 70% of dilution. At this condition, the combustion duration is on the limit of stability (CA10-90 around 45 CAD), thus further increments of the dilution rate should lead to misfire and unstable operation. This threshold is slightly lower than that suggested by the chemical simulations, but considering their simplicity, they can be accepted as a first approach for the concept assessment. Although not included, it is worth to mention that similar trends were observed at different loads (4 and 25 bar of IMEP).

Increasing the duration of combustion will lead to advance ignition to partially recover indicated performance during ST optimization in section 4.3. To consider a more realistic behaviour than keeping ST, the spark timing was modified

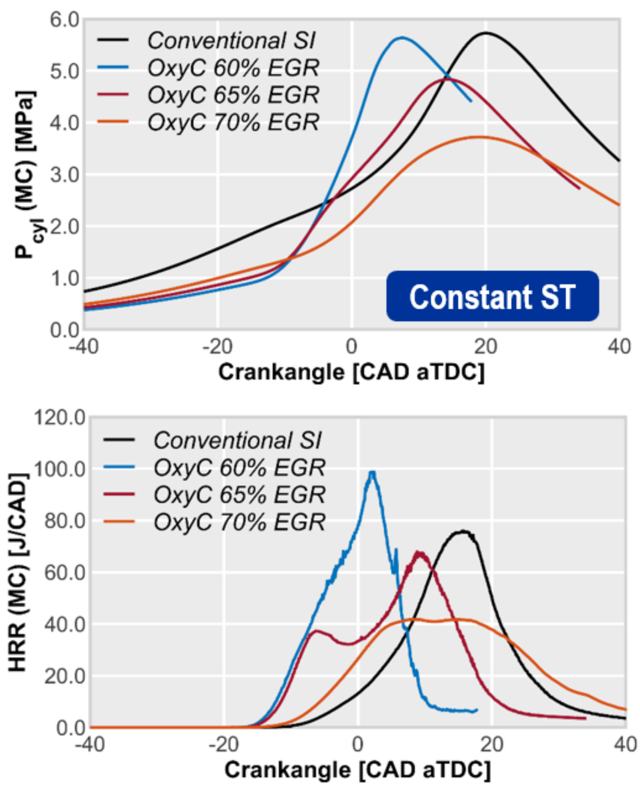

Figure 10: In-cylinder pressure signals (top) and HRR profiles (bottom) at 3000@11 for different EGR dilution rates at constant ST.

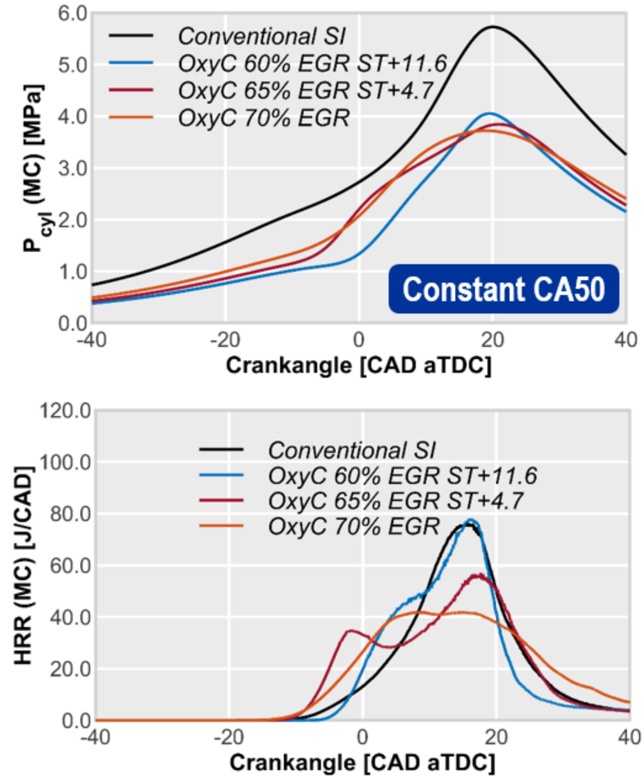

Figure 11: *In-cylinder pressure signals (top) and HRR profiles (bottom) at 3000@11 for different EGR dilution rates at constant CA50.*

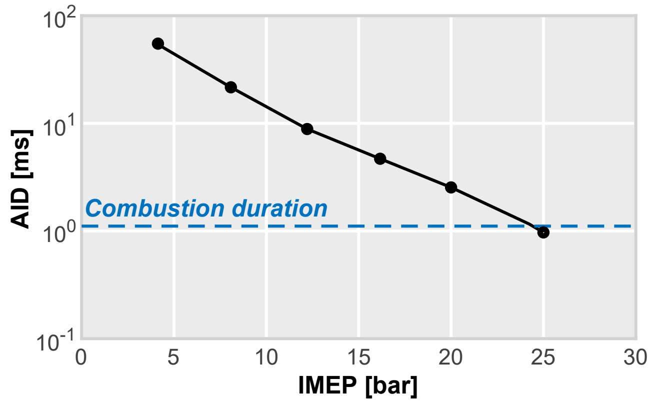

Figure 12: *Evolution of AID against the engine load. A reference combustion duration is included for time-scales comparison.*

to maintain the same combustion centring for the three EGR levels considered. In Fig. 11, results show a similar trends as the previous cases discussed in terms of combustion duration. The sensitivity to the dilution is also remarkable when CA50 is kept, even though lower than the effect seen for constant ST, thus maximum peak decreases about 40 J/CAD between extreme conditions considered. In addition, both the maximum heat release and the combustion duration are similar to those of conventional combustion when considering 60% of dilution. Through this analysis a more accurate EGR limit range was obtained, where the oxy-fuel combustion concept can operate. It should be noted that this range is similar to the one predicted with the 0D model, reinforcing this methodology to characterize the combustion concept in ICE applications.

4.2.2. *Knocking issues at full load operation*

Although chemical simulations demonstrated that a pure EGR dilution strategy keeps the knocking issues under control when oxy-fuel combustion is applied at low to medium engine loads, the risk of knocking combustion at full load conditions has not been evaluated so far.

In order to identify realistic conditions where knocking combustion is a critical problem, additional simulations were performed considering the conventional SI concept. In Fig. 12, the AID time is plotted for different engine loads ranging from 4 to 25 bar of IMEP. Boundary conditions were estimated from data of Table 4 and thermodynamic assumptions. In addition to the AID time of the mixture, the characteristic duration of combustion is included in this figure for comparison of time scales. As it can be seen, AID times are well above the characteristic combustion duration (≈20 CAD) in almost the whole load range. Nonetheless, both time scales become closer when the load increases above 20 bar of IMEP. At 25 bar of IMEP, the AID is lower than the combustion duration, thus the risk of knocking is clearly higher.

An equivalent oxy-fuel combustion operating point was simulated considering 25 bar of IMEP, where conventional SI combustion evinces a clear knock propensity. Results of this simulation are shown in Fig. 13. Here the in-cylinder pressure and HRR profile are plotted for a reference spark timing of -19 CAD aTDC. In addition, the original ST was shifted for GIE optimization (ST = -32.5 CAD) and results are also included in the same figure. the absence of knock, even at extreme ST advances, corroborates the findings obtained after the analysis of chemical simulations performed in section 3.2 for lower engine load conditions. Thus, diluting with high EGR rates (above 65%) seems to be a suitable strategy for oxy-fuel combustion since not only allows an stable and flexible engine operation but also guarantees the engine integrity.

4.3. *Assessment of oxy-fuel combustion performance*

Once the stability and safety thresholds are well established, the oxy-fuel combustion concept will be analysed in terms of engine outputs. In particular, the instantaneous in-cylinder pressure and temperature were predicted for an optimal spark advance and different dilutions with EGR. Moreover, other parameters related to the engine performance, such as the gross indicated efficiency, or the suitability of the exhaust temperatures for the MIEC operation, are also analysed.

Figure 14 shows the in-cylinder gas pressure and temperature operating at 3000@11, stoichiometric conditions and 70% of EGR dilution, both obtained by the coupling method

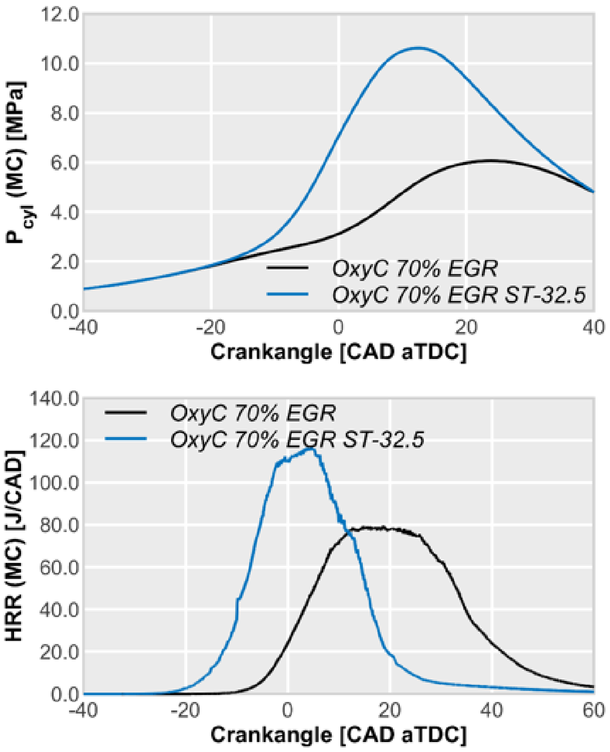

Figure 13: *In-cylinder pressure signals (top) and HRR profiles (bottom) at 3000@25 for different spark timings at 70% of EGR dilution rate.*

of 0D-1D and CFD. The significant reduction in pressure observed throughout the engine cycle can be explained because of several causes:

- Since the oxidizer is diluted by 70% (mass fraction) of inert gas (EGR) in oxy-fuel combustion and by 77% of N_2 (average mass fraction of dry air) in conventional combustion, a lower mass flow rate of oxidizer though the engine is required for keeping the same oxidizer-fuel ratio (i.e. stoichometric conditions). Therefore, the trapped mass in the cylinder at the valves closing is lower when considering oxy-fuel combustion.

- Similarly, if the fuel mass, the oxidizer-fuel ratio ($\lambda = 1$) and the dilution of the oxidizer are maintained between both combustion concepts, a lower intake pressure is required for achieving an equivalent oxy-fuel combustion operation. Since the EGR gas constant is lower than the N_2, the density of the oxidizer is higher if intake pressure and temperature are kept when the engine operates in oxy-fuel combustion mode, and thus pressure required to have the same mass flow rate though the engine is lower according to:

$$p_{\text{intake}} = p_0 = \rho \cdot R \cdot T_0 \tag{1}$$

- Furthermore, the adiabatic expansion coefficient (γ) when operating with EGR as the oxidizer diluent is lower than considering pure N_2. This aspect strongly conditions the pressure increase during the compression stroke, leading to a lower pressure increase.

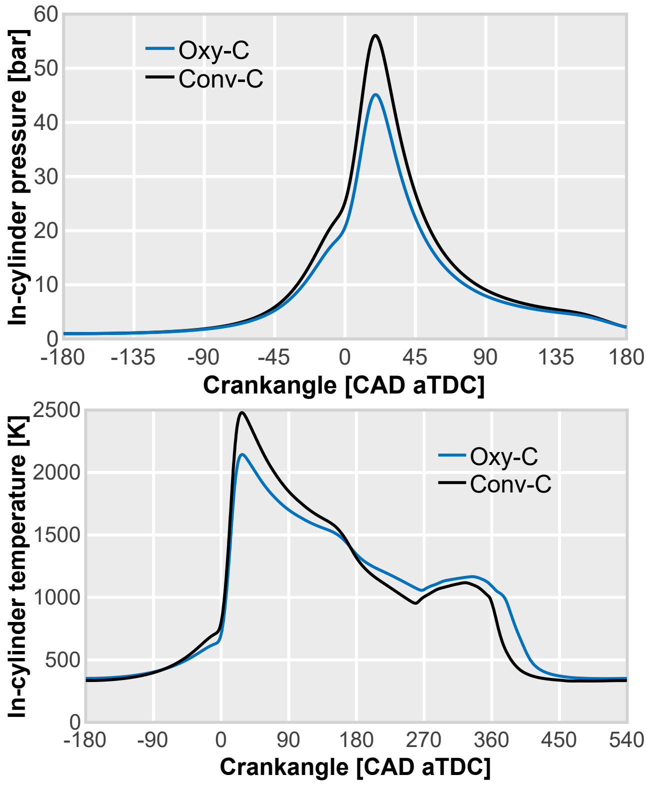

Figure 14: *Comparison between oxy-fuel combustion with 70% EGR dilution and conventional SI combustion concepts. In-cylinder pressure and temperature at 3000 rpm and 11 bar IMEP and $\lambda = 1$.*

Same trends can be observed in Fig. 15, where in-cylinder pressure and temperature are depicted for the low load operating condition (3000@4).

The effect of temperature during the compression is moderate since the intake temperature is kept constant when the combustion mode is changed. The small increase at IVC is given by the different intake and exhaust processes that are increasing the residual gases that remains in the cylinder after the scavenge process. In any case, the effect of the lower γ can be seen clearly during the compression stroke, where a lower temperature is reached right before the start of combustion in comparison with conventional combustion. During combustion, the change in the heat release law observed in Fig. 11 along with the higher specific heat of the diluent leads to a lower maximum temperature when the engine operates with oxy-fuel combustion. However, the effect of the lower γ during the expansion increases the temperature at exhaust valve opening in oxy-fuel combustion mode. This effect is interesting from the point of view of the O_2 production in the MIEC, but it must be controlled to not exceed the thermal limits of the engine components.

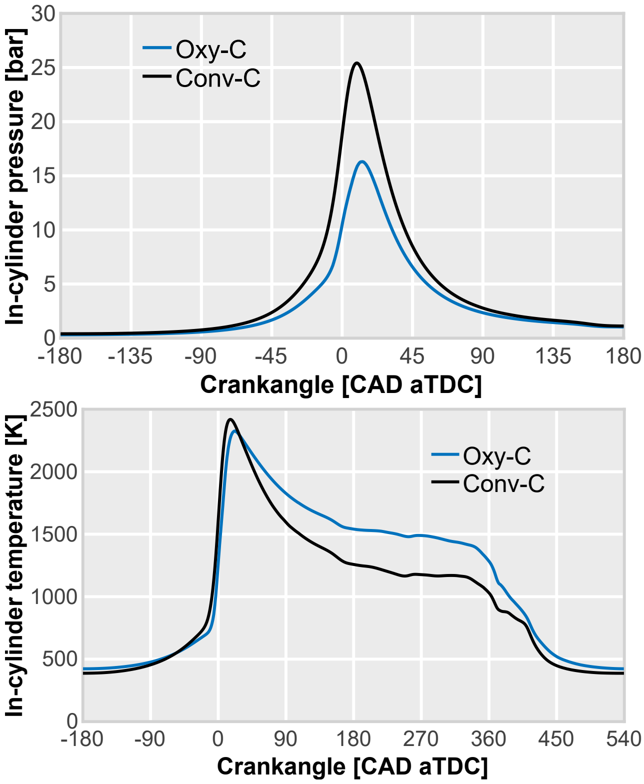

Figure 15: *Comparison between oxy-fuel combustion and conventional SI combustion concepts. In-cylinder pressure and temperature at 3000 rpm and 4 bar IMEP.*

Table 5 shows intake pressure, exhaust temperature and GIE values obtained for points 1 and 2 (see Table 4) operating with both combustion concepts. In both cases, stoichometric conditions are maintained and the ST was optimized according to the method described previously. For oxy-fuel combustion cases, the dilution rate was fixed at 70%.

Focusing on oxy-fuel combustion cases, the intake pressure and the exhaust temperature increases around 0.4 bar and 110 K, respectively, when switching from 4 to 11 bar of IMEP. In terms of performance, it is shown an improvement of around 1% when the load increases. Temperature differences are larger if both combustion concepts are compared, for instance, an increase of approximately 150 and 220 K is observed when switching form conventional to oxy-fuel combustion in point 1 and 2 respectively.

The variation observed in the boundary conditions and gas properties will affect the indicated efficiency when operating with oxy-fuel combustion. Thus, taking into account that γ is an important parameter for determining the performance in an ideal thermodynamic cycle (as it is well known from ideal Otto cycle analysis), the drop of around 8% at both operating points (3000@4 and 3000@11) can be explained mainly by the γ reduction, along with the changes in the combustion rate.

The effect of EGR on the combustion process has been studied before in section 4.2.1, but its specific impact on the engine outputs has not been assessed yet. Therefore, an additional study was performed to better understand the impact that the EGR dilution has in the oxy-fuel combustion operation. To this end, different levels of EGR dilution (60%, 65% and 70%) are simulated at point 2 (3000@11) maintaining the same CA50 in order to perform a fair and straightforward comparison.

Table 5: *Oxy-fuel combustion load assessment operating with 70% of EGR.*

	Conventional SI		Oxy-fuel combustion	
IMEP [bar]	4	11	4	11
Intake pressure [bar]	0.411	1.005	0.303	0.739
Exhaust temperature [K]	957	1004	1110	1220
GIE [%]	40.0	40.3	31.5	32.3

Figure 16 shows the instantaneous pressure evolution of these oxy-fuel cases together with the equivalent condition operating at conventional SI combustion. The maximum peak pressures values reached are similar in the three oxy-fuel combustion cases. The effect of the combustion slowdown evinced in Fig. 11 on the pressure evolution is compensated somehow by the increased pressure during the compression stroke as the EGR rate increases. This pressure increase is explained by the increment of intake pressure required to reach the target EGR rate, while keeping the oxidizer-fuel ratio.

Regarding the gas temperature,it decreases as the dilution with EGR increases, mainly due to the fact that trapped mass of diluted gas in the cylinder is higher. For this reason, lower EGR dilution rates lead to higher temperatures at the valves opening and thereby, to higher exhaust temperatures. This is an important aspect to take into account since the membrane functioning is strongly dependent on this parameter. Therefore, the control of the EGR rate could be an interesting strategy not only for assuring both the combustion stability and the engine integrity, but also to optimize the MIEC operation.

The stated changes in the engine operation produce the GIE trends observed in Fig. 17. As it can be seen, there is an improvement of 1.1% when EGR dilution increase from 60% to 70%, thus confirming the expected trend when both CO_2 and H_2O concentrations get larger. The reduction of heat rejection due to the lower temperatures in the cylinder explains this trend. Although this is a notable increment, GIE values are far from the levels offered by the conventional SI combustion. This is the main disadvantage of the oxy-fuel combustion, however it must be highlighted that it is compensated by the suitability and potential of the oxy-fuel combustion to facilitate the CO_2 capture thanks to the absence of N_2 in the exhaust gases.

5. Conclusions

A numerical method, validated with engine experiments, has been developed to verify the viability of the oxy-fuel combustion for SI homogeneous combustion concept in a recip-

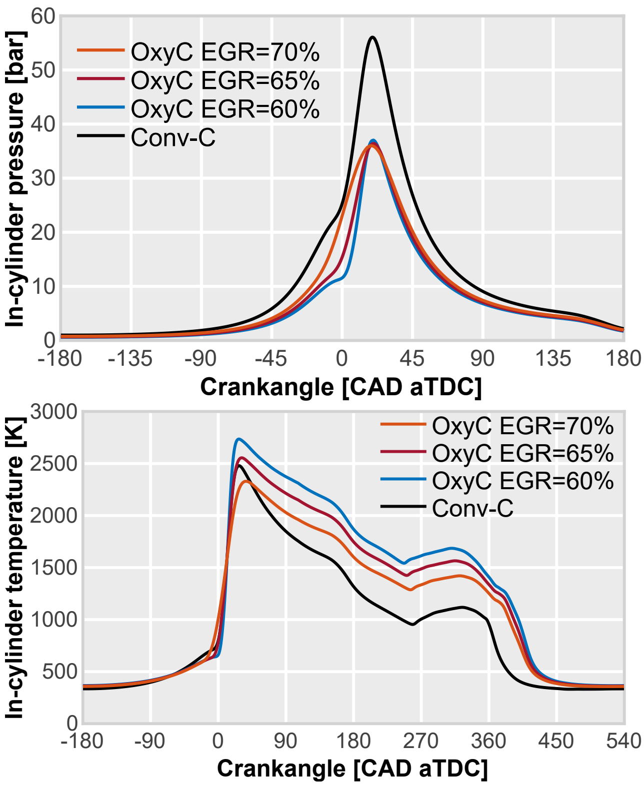

Figure 16: *Effect of EGR dilution on the in-cylinder pressure and temperature at 3000 rpm, 11 bar IMEP using oxy-fuel combustion.*

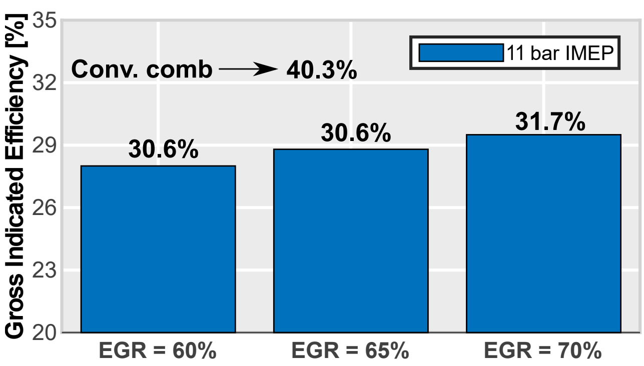

Figure 17: *GIE at 3000 rpm and 11 bar of IMEP at constant CA50.*

rocating ICE operating under realistic conditions. Since results reproduce well the trends observed in the engine experiments, the following conclusions can be drawn:

- The combination of simple chemical simulations with some thermodynamic assumptions helps to provide a realistic prediction of safety and stability thresholds for oxy-fuel combustion operation. These results have been considered as first estimation, since they slightly change when simulations with higher accuracy are performed.

- EGR dilution strategy is intrinsically more appropriate for an integrated oxy-fuel combustion concept. Using a oxygen-based dilution strategy, the O_2 MIEC production should be significantly increased to achieve conditions comparable to a pure EGR dilution strategy. In addition, it is technologically easier to recirculate the exhaust gases. And will be easier to liquefy for storage and capture at supercritical conditions the CO_2.

- In this way, the engine should be operated near-stoichometric conditions ($\lambda \approx 1$) with EGR dilution rates ranged between 60% and 70% to avoid, on the one hand, exceeding in-cylinder thermo-mechanical limits and engine knocking, and on the other hand ensuring the combustion stability. In should be note, that in order to achieve higher levels of dilution without getting stability issues (and also interesting from the point of view of the thermal efficiency), the spark timing must be optimized.

- The oxy-fuel combustion concept is expected to be more flexible in terms of spark advance at high load condition (where this abnormal combustion should compromise the optimum combustion phasing in conventional SI combustion), since no knocking issues are expected in a wide range of spark timing.

- An important reduction of the indicated efficiency is expected when the engine operates in oxy-fuel combustion mode (around 8 percentual points less at equivalent operating conditions), also compromising the brake specific fuel consumption. Nevertheless, despite this penalty in fuel consumption, the oxy-fuel combustion concept is really advantageous when integrates a MIEC for in-situ O_2 production, since it allows easily implementing techniques for CO_2 capturing, and therefore not any CO_2 will be released into the atmosphere. It means that the link between engine efficiency and CO_2 emissions could be broken.

- The EGR operating range is closely constrained by thermo-mechanical limits due to the resistance of materials and combustion stability, this narrow range (maximum range between 60% and 70%) might be challenging for control purposes.

- On the other hand, as no knocking issues are expected, even at full load conditions with extremely advanced spark timings, increasing the compression ratio could be an interesting strategy for recovering part of the thermal efficiency reduction when the oxy-fuel concept is applied. It must be taken into account that even thought the CO2 can be captured, increasing the efficiency is important to reduce the costs.

Funding

This research was partially supported by Agència Valenciana de la Innovació (AVI) through the project "Demostrador de un motor de oxicombustión con captura de CO_2" INNVA1 /2021/38.

Acknowledgements

The authors want to express their gratitude to CONVERGENT SCIENCE Inc. and Convergent Science GmbH for their kind support for the 0D, 1D, and CFD calculations with the CONVERGE software.

The authors would like to thank Ing. Gabriel Alcantarilla Ballesteros for his inestimable work during the experimental campaign.

References

[1] European Commission, COM(2014) 15 final: A policy framework for climate and energy in the period from 2020 to 2030 (2014).

[2] European Commission, Determining the environmental impacts of conventional and alternatively fuelled vehicles through LCA (2020).

[3] European Commission, COM(2019) 38 final: Amending Regulation (EU) 2015/757 in order to take appropriate account of the global data collection system for ship fuel oil consumption data (2019).

[4] C. Beck, J. Schorr, H. Echtle, J. Verhagen, A. Jooss, C. Krüger, M. Bargende, Numerical and experimental investigation of flow phenomena in rotating step-holes for direct-spray-cooled electric motors, International Journal of Engine Research 22 (5) (2021) 1731–1740.

[5] P. R. Hooper, Low noise, vibration and harshness solutions for in-line three-cylinder range extender and hybrid electric vehicles, International Journal of Engine Research 22 (2) (2021) 581–591.

[6] A. Solouk, J. Tripp, M. Shakiba-Herfeh, M. Shahbakhti, Fuel consumption assessment of a multi-mode low temperature combustion engine as range extender for an electric vehicle, Energy Conversion and Management 148 (2017) 1478–1496.

[7] A. Broatch, J. Serrano, F. Arnau, D. Moya, Time-domain computation of muffler frequency response: comparison of different numerical schemes, Journal of sound and vibration 305 (1-2) (2007) 333–347.

[8] J. Galindo, J. R. Serrano, P. Piqueras, Ó. García-Afonso, Heat transfer modelling in honeycomb wall-flow diesel particulate filters, Energy 43 (1) (2012) 201–213.

[9] A. Broatch, P. Olmeda, X. Margot, J. Gomez-Soriano, A one-dimensional modeling study on the effect of advanced insulation coatings on internal combustion engine efficiency, International Journal of Engine Research (2020) 1468087420921584.

[10] J. Benajes, R. Novella, J. Gomez-Soriano, P. Martinez-Hernandiz, C. Libert, M. Dabiri, Evaluation of the passive pre-chamber ignition concept for future high compression ratio turbocharged spark-ignition engines, Applied Energy 248 (2019) 576–588.

[11] A. Van Blarigan, D. Kozarac, R. Seiser, J. Chen, R. Cattolica, R. Dibble, Spark-ignited engine nox emissions in a low-nitrogen oxycombustion environment, Applied Energy 118 (2014) 22–31.

[12] C. Liu, G. Chen, N. Sipöcz, M. Assadi, X. Bai, Characteristics of oxy-fuel combustion in gas turbines, Applied Energy 89 (1) (2012) 387–394.

[13] S. K. Park, T. S. Kim, J. L. Sohn, Y. D. Lee, An integrated power generation system combining solid oxide fuel cell and oxy-fuel combustion for high performance and CO2 capture, Applied Energy 88 (4) (2011) 1187–1196.

[14] Q. Tan, Y. Hu, A study on the combustion and emission performance of diesel engines under different proportions of O2 N2 CO2, Applied Thermal Engineering 108 (2016) 508–515.

[15] Z. Kang, Z. Wu, Z. Zhang, J. Deng, Z. Hu, L. Li, Study of the Combustion Characteristics of a HCCI Engine Coupled with Oxy-Fuel Combustion Mode, SAE International Journal of Engines 10 (3) (2017).

[16] S. Chen, Y. Zheng, M. Wu, J. Hu, W. Xiang, Thermodynamic analysis of oxy-fuel combustion integrated with the sco2 brayton cycle for combined heat and power production, Energy Conversion and Management 232 (2021) 113869.

[17] X. Wei, V. Manovic, D. P. Hanak, Techno-economic assessment of coal- or biomass-fired oxy-combustion power plants with supercritical carbon dioxide cycle, Energy Conversion and Management 221 (2020) 113143.

[18] X. Pei, B. He, L. Yan, C. Wang, W. Song, J. Song, Process simulation of oxy-fuel combustion for a 300mw pulverized coal-fired power plant using aspen plus, Energy Conversion and Management 76 (2013) 581–587.

[19] F. Carrasco-Maldonado, R. Spörl, K. Fleiger, V. Hoenig, J. Maier, G. Scheffknecht, Oxy-fuel combustion technology for cement production - State of the art research and technology development, International Journal of Greenhouse Gas Control 45 (2016) 189–199.

[20] A. I. Escudero, S. Espatolero, L. M. Romeo, Oxy-combustion power plant integration in an oil refinery to reduce CO2 emissions, International Journal of Greenhouse Gas Control 45 (2016) 118–129.

[21] S. Baumann, J. M. Serra, M. P. Lobera, S. Escolástico, F. Schulze-Küppers, W. A. Meulenberg, Ultrahigh oxygen permeation flux through supported Ba0.5Sr0.5Co0.8Fe0.2O3-δ membranes, Journal of Membrane Science 377 (1-2) (2011) 198–205.

[22] D. Catalán-Martínez, A. Santafé-Moros, J. M. Gozálvez-Zafrilla, J. García-Fayos, J. M. Serra, Characterization of oxygen transport phenomena on BSCF membranes assisted by fluid dynamic simulations including surface exchange, Chemical Engineering Journal 387 (2020).

[23] F. J. Arnau, J. V. Benajes, D. Catalán, J. M. Desantes, L. M. García-Cuevas, J. M. Serra, J. R. Serrano, Internal combustion engine and operating method of the same. motor de combustión interna y método de funcionamiento del mismo, p201930285, 28.03.2019. WO2020/193833A1, 01.10.2020. PCT/ES2020/070199, 21.03.2020. ES2751129B2, 29.03.2021.

[24] J. Benajes, P. Olmeda, J. Martín, R. Carreño, A new methodology for uncertainties characterization in combustion diagnosis and thermodynamic modelling, Applied Thermal Engineering 71 (1) (2014) 389–399.

[25] F. Payri, P. Olmeda, J. Martin, R. Carreño, A New Tool to Perform Global Energy Balances in DI Diesel Engines, SAE International Journal of Engines 7 (1) (2014) 43–59.

[26] R. Bounaceur, P.-A. Glaude, B. Sirjean, R. Fournet, P. Montagne, M. Vierling, M. Moliere, Prediction of auto-ignition temperatures and delays for gas turbine applications, Journal of Engineering for Gas Turbines and Power 138 (2016) 021505.

[27] Y.-D. Liu, M. Jia, M.-Z. Xie, B. Pang, Enhancement on a skeletal kinetic model for primary reference fuel oxidation by using a semidecoupling methodology, Energy & Fuels 26 (12) (2012) 7069–7083.

[28] J. Benajes, R. Novella, J. Gomez-Soriano, I. Barbery, C. Libert, F. Rampanarivo, M. Dabiri, Computational assessment towards understanding the energy conversion and combustion process of lean mixtures in passive pre-chamber ignited engines, Applied Thermal Engineering 178 (2020) 115501.

[29] K. Fieweger, R. Blumenthal, G. Adomeit, Self-ignition of si engine model fuels: a shock tube investigation at high pressure, Combustion and Flame 109 (4) (1997) 599–619.

[30] M. Metghalchi, J. C. Keck, Burning velocities of mixtures of air with methanol, isooctane, and indolene at high pressure and temperature, Combustion and flame 48 (1982) 191–210.

[31] Ö. L. Gülder, Correlations of laminar combustion data for alternative si engine fuels, Tech. rep., SAE Technical Paper (1984).

[32] S. Jerzembeck, N. Peters, P. Pepiot-Desjardins, H. Pitsch, Laminar burning velocities at high pressure for primary reference fuels and gasoline: Experimental and numerical investigation, Combustion and Flame 156 (2) (2009) 292–301.

[33] S. Heimel, R. C. Weast, Effect of initial mixture temperature on the burning velocity of benzene-air, n-heptane-air, and isooctane-air mixtures, in: Symposium (international) on combustion, Vol. 6, Elsevier, 1957, pp. 296–302.

[34] P. Olmeda, J. Martín, R. Novella, D. Blanco-Cavero, Assessing the optimum combustion under constrained conditions, International J of Engine Research 21 (5) (2020) 811–823.

[35] P. Olmeda, J. Martín, F. J. Arnau, S. Artham, Analysis of the energy balance during world harmonized light vehicles test cycle in warmed and cold conditions using a virtual engine, International J of Engine Research 21 (6) (2020) 1037–1054.
[36] CONVERGENT SCIENCE Inc., CONVERGE 2.4 Theory Manual (2018).
[37] V. Yakhot, S. A. Orszag, Renormalization group analysis of turbulence. i. basic theory, Journal of scientific computing 1 (1) (1986) 3–51.
[38] A. Broatch, R. Novella, J. García-Tíscar, J. Gomez-Soriano, P. Pal, Investigation of the effects of turbulence modeling on the prediction of compression-ignition combustion unsteadiness, International Journal of Engine Research (2021) 1468087421990478.
[39] C. Angelberger, T. Poinsot, B. Delhay, Improving near-wall combustion and wall heat transfer modeling in si engine computations, Tech. rep., SAE Technical Paper (1997).
[40] R. Cant, Sb pope, turbulent flows, cambridge university press, cambridge, uk, Combustion and Flame 125 (2001) 1361–1362.
[41] A. J. Torregrosa, A. Broatch, X. Margot, J. Gomez-Soriano, Understanding the unsteady pressure field inside combustion chambers of compression-ignited engines using a computational fluid dynamics approach, International Journal of Engine Research 21 (8) (2020) 1273–1285.
[42] R. I. Issa, Solution of the implicitly discretised fluid flow equations by operator-splitting, Journal of computational physics 62 (1) (1986) 40–65.
[43] P. Senecal, E. Pomraning, K. Richards, T. Briggs, C. Choi, R. McDavid, M. Patterson, Multi-dimensional modeling of direct-injection diesel spray liquid length and flame lift-off length using cfd and parallel detailed chemistry, SAE transactions (2003) 1331–1351.
[44] A. Babajimopoulos, D. Assanis, D. Flowers, S. Aceves, R. Hessel, A fully coupled computational fluid dynamics and multi-zone model with detailed chemical kinetics for the simulation of premixed charge compression ignition engines, International journal of engine research 6 (5) (2005) 497–512.
[45] R. Scarcelli, N. Matthias, T. Wallner, Numerical investigation of combustion in a lean burn gasoline engine, SAE Technical Paper (2013).
[46] P. Pal, D. Probst, Y. Pei, Y. Zhang, M. Traver, D. Cleary, S. Som, Numerical investigation of a gasoline-like fuel in a heavy-duty compression ignition engine using global sensitivity analysis, SAE International Journal of Fuels and Lubricants 10 (1) (2017) 56–68.
[47] X. Yang, A. Solomon, T.-W. Kuo, Ignition and combustion simulations of spray-guided sidi engine using arrhenius combustion with spark-energy deposition model, SAE Technical Paper (2012).
[48] A. Torregrosa, P. Olmeda, B. Degraeuwe, M. Reyes, A concise wall temperature model for di diesel engines, Applied Thermal Engineering 26 (11-12) (2006) 1320–1327.
[49] J. Benajes, R. Novella, J. Gomez-Soriano, I. Barbery, C. Libert, Advantages of hydrogen addition in a passive pre-chamber ignited si engine for passenger car applications, International Journal of Energy Research.
[50] L. M. García-Cuevas, F. Arnau, R. Novella, F. Gutiérrez, Adapting an internal combustion engine to oxy-fuel combustion with in-situ oxygen production, ASME - ICEF. The Internal Combustion Engine Fall Conference. Virtual Conference, Online: October 13 - 15, 2021 (Under review).

Nomenclature

AID	Auto ignition delay
AMR	Adaptive mesh refinement
BSFC	Brake specific fuel consumption
CAD	Crank angle degree
CCS	Carbon capture storage
CFD	Computational fluid dynamics
HC	Hydrocarbons
CO	Carbon oxides
EGR	Exhaust gas recirculation
EU	European Union
FPI	Fuel port injection
GIE	Gross indicated efficiency
HRR	Heat release rate
ICE	Internal combustion engine
IMEP	Indicated mean effective pressure
IVC	Inlet valve closing
MIEC	Mixed ionic-electronic conducting
MZ	Multi zone
NOx	Nitrogen oxides
PID	Proportional, integration and derivative
PISO	Pressure implicit with splitting of operators
PRF	Primary reference fuel
RNG	Re-normalization group
SA	Spark advance
SI	Spark ignition
ST	Spark timing
URANS	Unsteady Reynolds-averaged Navier–Stokes